DOI: 10.1002/smll.200600070

Materials Specificity and Directed Assembly of a Gold-Binding Peptide

*Candan Tamerler, Memed Duman, Ersin Emre Oren, Mustafa Gungormus, Xiaorong Xiong, Turgay Kacar, Babak A. Parviz, and Mehmet Sarikaya**

***A**dsorption studies of a genetically engineered gold-binding peptide, GBP1, were carried out using a quartz-crystal microbalance (QCM) to quantify its molecular affinity to noble metals. The peptide showed higher adsorption onto and lower desorption from a gold surface compared to a platinum substrate. The material specificity, that is, the preferential adsorption, of GBP1 was also demonstrated using gold and platinum micropatterned on a silicon wafer containing native oxide. The biotinylated three-repeat units of GBP1 were preferentially adsorbed onto gold regions delineated using streptavidin-conjugated quantum dots (SAQDs). These experiments not only demonstrate that an inorganic-binding peptide could preferentially adsorb onto a metal (Au) rather than an oxide (SiO_2) but also onto one noble metal (Au) over another (Pt). This result shows the utility of an engineered peptide as a molecular erector in the directed immobilization of a nanoscale hybrid entity (SAQDs) over selected regions (Au) on a fairly complex substrate (Au and Pt micropatterned regions on silica). The selective and controlled adsorption of inorganic-binding peptides may have significant implications in nano- and nanobiotechnology, where they could be genetically tailored for specific use in the development of self-assembled molecular systems.*

Keywords:
- cross-specificity
- directed assembly
- peptide binding
- protein engineering
- quantum dots

1. Introduction

Biological materials are formed via the templating of proteins that may control nucleation, morphogenesis, and the synthesis of hard tissue such as the skeletons of single- and multi-celled organisms with complex architectures.[1–3] The biological processes through which organisms control and monitor tissue formation are due to the molecular recognition and the self- and co-assembly of proteins with inorganic materials that are involved in biomineralization; organisms acquire these characteristics through millions of years of evolution.[3] Biogenic materials, such as metals (gold, silver, etc.), ceramics (silica, hydroxyapatite, calcite, aragonite, and magnetite), and semiconductors (cadmium sulfide and iron sulfide), of different physical properties, for example, mechanical, electronic, optical, and magnetic, are fabricated under mild conditions of neutral pH, ambient

[*] Prof. C. Tamerler, M. Duman, Dr. E. E. Oren, M. Gungormus, T. Kacar, Prof. M. Sarikaya
Materials Science & Engineering Department
Roberts Hall, Box: 352120
University of Washington
Seattle, WA 98195 (USA)
Fax: (+1) 206-543-3100
E-mail: sarikaya@u.washington.edu
Prof. C. Tamerler, M. Gungormus, T. Kacar
Molecular Biology & Genetics
Istanbul Technical University
Maslak 80626, Istanbul (Turkey)
X. Xiong, Prof. B. A. Parviz
Electrical Engineering Department,
University of Washington
Seattle, WA 98195 (USA)

NANO MICRO small

temperature, and in aqueous solution.[3–5] Using biomolecular pathways similar to nature's, it is desirable to produce technologically relevant materials with precision and specific control of fabrication by using inorganic-recognizing proteins or peptides.[6] In addition, these biomolecules could be further structurally designed to introduce tailored functionalities, such as material-specific binding, using genetic engineering protocols for particular applications.[6] Adapting molecular biology pathways to materials science now allows the combinatorial selection of peptides with an affinity to specific inorganic materials.[7–10] Once selected, these inorganic-binding peptides could be used to create hybrid systems as molecular linkers in nano- and nanobiotechnology, as immobilizers in biogenic thin films to create biocompatible materials, and as growth-modifier biomineralization agents in tissue engineering and new hybrid materials.[6–9]

There is increasing interest in the selection and utilization of inorganic-binding peptides for a wide range of applications.[6–10] These peptides, called genetically engineered peptides for inorganics (GEPI), are selected using bacterial-cell-surface and phage-display protocols for their affinity to various inorganic surfaces including powders, single crystals, and nanoparticles. Once a GEPI is selected, however, it is necessary to have a better understanding of its binding affinity with a given inorganic material so that it can be utilized appropriately in a variety of applications or so that its functional property can be further tailored. A peptide's affinity for a material may be determined through its adsorption strength onto that specific material for which the peptide was selected. Furthermore, the peptide's selective adsorption to the given material compared to other materials of interest is crucial in terms of determining its cross-specificity, essential when the peptide is used in complex, multimaterial applications. Therefore, quantitative analysis of peptide adsorption kinetics and the thermodynamics of inorganic surfaces is necessary to assess a peptide's characteristics that lead to its robust performance in material assembly and fabrication.

Here we report the first quantitative demonstration of the material affinity and cross-specificity of a cell-surface-display-selected and post-selection engineered inorganic-binding peptide, namely a gold-binding peptide, GBP1.[11] The specificity of the gold-binding peptide was assessed on two noble metals, gold and platinum, by using a quartz-crystal microbalance (QCM) to delineate the differences in its binding affinities to different materials. To demonstrate the utility of the peptide for directing the assembly of nanoscale objects on predefined locations, a template consisting of a silicon dioxide background and a pattern of parallel gold lines was fabricated to assess noble-metal versus oxide cross-selectivity; gold and platinum patterns were then microfabricated onto a SiO_2-covered wafer to assess cross-selectivity between the two noble metals. The selective self-assembly of the biotinylated gold-binding peptide was verified by using streptavidin-conjugated quantum dots (SAQD) and observing the resulting fluorescence on the microfabricated template. Our results are significant in two fundamental areas. Firstly, the genetically engineered peptides offer a new pathway in the investigation of the nature of the peptide/protein–inorganic interaction and provide the essential information that has eluded the fields of biomineralization, tissue regeneration, and creation of biocompatible surfaces.[12–14] Secondly, peptides binding specifically to desired inorganics are practical molecular entities for the development of new, highly biofunctional platforms for peptide-based chips for use in areas ranging from biosensors to proteomics.[15–17]

2. Results and Discussion

2.1. Adsorption of a Gold-Binding Peptide onto Metallic Gold and Platinum Substrates: A Quantitative Comparison

The gold-binding peptide, GBP1, was originally selected from a cell-surface-display library, in which the randomized foreign gene product was displayed in the extracellular loops of an outer membrane protein, maltoporin, that was fused to the amino terminus of the alkaline phosphatase with the retention of gold-binding activity.[11] Experimental studies indicated that a strong binding property is presented by the three-repeat sequence MHGKTQATSGTIQS (3R-GBP1).[11] We adapted QCM spectroscopy to quantitatively characterize the inorganic-binding peptide adsorption behavior under various solution conditions. The QCM is a sensitive mass-measurement device and can monitor the kinetics and thermodynamics of the molecular binding processes on any material that can be coated onto a quartz crystal.[18–19] Depending on the degree of molecular adsorption (or desorption) from solution onto the quartz crystal, the change in the frequency of the mechanical oscillator can be correlated with the amount of mass on the substrate surface as a function of time.[20] The change in the crystal frequency at different concentrations of GBP1 on the gold and platinum surfaces is shown in Figure 1 as a result of the QCM experiments. The figure shows that the frequency change for the adsorption of GBP1 onto each of the two metals fits well to the Langmuir 1:1 adsorption model.[21] In the frequency-difference profile, two distinct groups due to adsorption of 3R-GBP1 are observed, one for the gold and the other for the platinum electrode.

According to the Sauerbrey equation,[22] the change in the resonance frequency of the QCM is related to the mass absorbed onto the electrode surface. Although frequently used for studying the adsorption of molecular species on solid substrates submerged in liquids, this relationship was originally derived strictly for gas-phase mass deposition on substrates; complications may arise, therefore, for the liquid-phase molecular adsorption due to a number of parameters, including the complex dielectric response of the solvent,[23] the trapped and hydrated water in the molecular layer, viscoelastic effects in the adsorbed layer, and variations in the acoustic coupling of the molecule to the liquid.[24,25] Although any of these parameters may affect peptide adsorption onto noble metals, our primary objective here was to determine the rate of mass change associated with the formation of a 3R-GBP1 monolayer on both gold

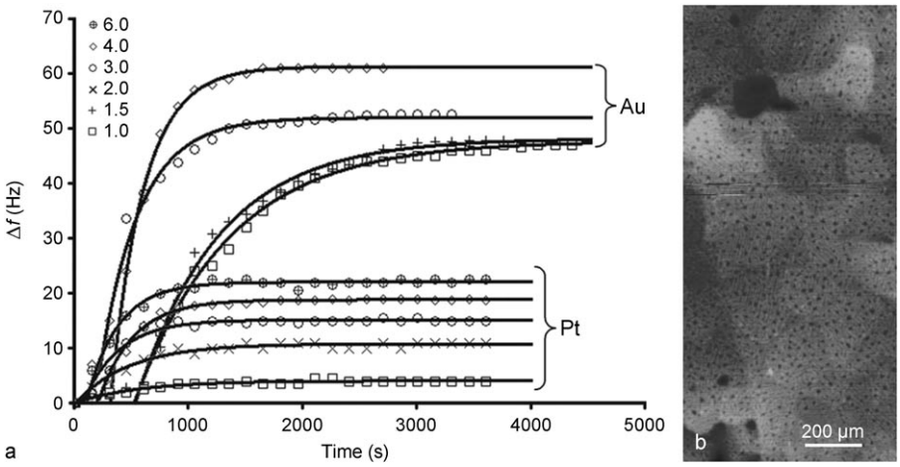

Figure 1. a) Frequency changes observed for different concentrations (μg mL^{-1}) of GBP1 on Au and Pt electrodes and their model fit (solid lines) based on Langmuir adsorption kinetics. Both correlations are plotted within a 95% confidence interval (C.I.) b) An atomic force microscopy (AFM) image showing the highly planar assembly of single-molecule-thick GBP1 on a (111)-oriented gold substrate.

and platinum rather than to extract the absolute change in mass.

The kinetic constants obtained for the adsorption/desorption process of 3R-GBP1 onto gold and platinum surfaces are given in Table 1. The values are calculated based on the rate of the surface reaction governed by the Langmuir isotherms, given by:[26]

$$\frac{d\theta}{dt} k_a(1-\theta)C - k_d\theta \quad (1)$$

where θ is the fraction of surface covered, C is the 3R-GBP1 concentration, and k_a and k_d are the association and dissociation constants, respectively. The monolayer formation over time is obtained by integrating the rate of the surface reaction.

$$\theta(t) = \frac{C}{C + k_d/k_a}[1 - \exp(-k_aC + k_d)t)] \quad (2)$$

Substitution of the expressions $k_{obs} = k_aC + k_d$ and $\theta(\infty) = C/(C+k_d/k_a)$ and the modification of t with $t - t_o$ to eliminate the mixing effects[26] gives:

$$\theta(t - t_0) = \theta(\infty)[1 - (- k_{obs}(t - t_0))] \quad (3)$$

The parameters of Equation (3) can be optimized by using a nonlinear regression method, with the result that the fitted lines and data points are produced as shown in Figure 2.

The values of $\theta(\infty)$ and k_{obs} were calculated for different concentrations of the peptide adsorbed onto a gold or platinum substrate with a 95% confidence interval (C.I.). The results are given in Table 1. Also, knowing that $k_{obs} = k_aC + k_d$, we could then plot C versus k_{obs} and obtain the best fits (with a 95% C.I.). Figure 2 shows two such best-fit lines corresponding to the concentration dependence of k_{obs} of 3R-GBP1 adsorbed onto gold and platinum, respectively. These lines have a slope of k_a and an intercept of k_d, giving the values of adsorption and desorption parameters, respectively, as shown in Table 2.

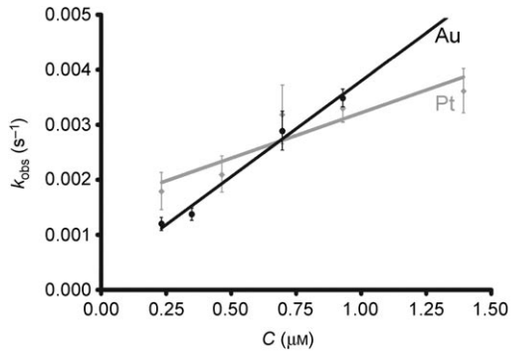

Figure 2. Concentration dependence of k_{obs} of 3R-GBP1 on Au and Pt electrodes. Both correlations are plotted within a 95% confidence interval.

Using the adsorption/desorption values obtained so far it is also possible to achieve a quantitative measurement of the energetics, another parameter used to assess the interfacial binding affinity of the molecule onto a given substrate. The binding strength of the polypeptide on a solid substrate can be obtained by estimating the standard Gibbs free energy of adsorption using the relationship $\Delta G_{ads} = -RT\ln(K_{eq}C)$, where K_{eq} is the equilibrium constant given by $K_{eq} = k_a/k_d$, T is temperature and R is the gas constant. The estimated molarity representations of the standard Gibbs free energy of adsorption of the GBP1 mono-

Table 1. $\theta(\infty)$ and k_{obs} values determined from raw data as a function of GBP1 concentration. C.I. = confidence interval.

Substrate	Concentration [μg mL^{-1}]	Concentration [M]	$k_{obs} \pm 95\%$ C.I. [s^{-1}]	$\theta(\infty) \pm 95\%$ C.I. [Hz]
Gold	1	0.23×10^{-6}	$(1.20 \pm 0.07) \times 10^{-3}$	47.63 ± 0.37
	1.5	0.35×10^{-6}	$(1.37 \pm 0.12) \times 10^{-3}$	48.10 ± 0.59
	3	0.70×10^{-6}	$(2.89 \pm 0.33) \times 10^{-3}$	51.87 ± 0.53
	4	0.93×10^{-6}	$(3.48 \pm 0.15) \times 10^{-3}$	61.17 ± 0.24
Platinum	1	0.23×10^{-6}	$(1.79 \pm 0.32) \times 10^{-3}$	4.04 ± 0.08
	2	0.46×10^{-6}	$(2.09 \pm 0.31) \times 10^{-3}$	10.77 ± 0.16
	3	0.70×10^{-6}	$(3.18 \pm 0.52) \times 10^{-3}$	15.16 ± 0.19
	4	0.93×10^{-6}	$(3.30 \pm 0.22) \times 10^{-3}$	18.81 ± 0.10
	6	1.39×10^{-6}	$(3.61 \pm 0.39) \times 10^{-3}$	22.04 ± 0.17

NANO MICRO small

Table 2. Parameters of adsorption kinetics of 3R-GBP1 on Au and Pt substrates. K_{eq} is the equilibrium constant.

Substrate	$k_a \pm 95\%$ C.I. [$M^{-1}s^{-1}$]	$k_d \pm 95\%$ C.I. [s^{-1}]	K_{eq} [M^{-1}]	ΔG_{ads} [kcal mol^{-1}]
Gold	$(3.49\pm0.30)\times10^{3}$	$(3.12\pm1.86)\times10^{-4}$	$(1.12\pm0.67)\times10^{7}$	-9.68 ± 0.28
Platinum	$(1.65\pm0.41)\times10^{3}$	$(1.57\pm0.35)\times10^{-3}$	$(1.05\pm0.35)\times10^{6}$	-8.27 ± 0.17

layer onto gold and platinum are given in Table 2. The errors in k_a and k_d were again calculated with a 95% C.I.; however, the errors in K_{eq} and ΔG_{ads} were determined by the propagation of the uncertainty in the k_a and k_d values. The levels of accuracy are consistent with those in the literature for molecular adsorption studies of, for example, self-assembled monolayers.[26]

A close inspection of the values in Table 2 reveals that the adsorption coefficient k_a of 3R-GBP1 on gold is twice that of platinum. Furthermore, the desorption constant k_d shows a significant order-of-magnitude difference in the binding of the peptide onto the two noble metal surfaces, that is, desorption from Au is significantly lower than from Pt. These kinetic constants indicate not only that GBP1 has a higher association for the gold surface but also that the polypeptide desorbs much more easily from the platinum than from the gold surface. Both of these parameters result in one order-of-magnitude difference in the equilibrium constant of 3R-GBP1 binding to gold compared to the value for binding to platinum. In addition, the free-energy values for adsorption of the peptide onto the two metal surfaces indicate that the interface is more stable when the GBP binds to the gold rather than to the platinum surface. In summary, the kinetic and thermodynamic values indicate that the peptide, originally combinatorially selected to bind to gold, adsorbs onto a gold substrate quickly, covers it readily (see below), and does not easily desorb.

The k_d values of adsorption of the 3R-GBP1 assembly onto both gold and platinum are positive and they are equilibrium systems. Therefore, for a given instant of time there are some unoccupied adsorption sites on both surfaces. Using the Langmuir isotherm analysis and the corresponding equilibrium constants, we can determine the steady-state (equilibrium) fractional surface coverage $\theta(\infty)$ of the gold-binding peptide onto each of the metal substrates through $\theta(\infty) = C/(C+K_{eq}^{-1})$. The obtained fractional steady-state-coverage data was plotted versus the concentration, as shown in Figure 3; the peptide covers the gold surface very rapidly compared to the platinum substrate. At very low concentrations (<0.1 μM), the ratio of the equilibrium surface-coverage value for Au versus Pt is about ten; this value drops to around two at high concentrations (>1 μM) and finally reaches unity at extreme concentrations (>100 μM). A gradual drop in coverage rate is expected because of the steric hindrance of the molecules on the adsorbed surface. Our subsequent experiment (see below) involving the directed adsorption and material specificity of the peptide onto gold versus platinum used a 0.12-μM (0.5 μg mL^{-1}) 3R-GBP1 concentration because of the significant difference (fivefold) in the equilibrium surface coverage of the peptide on platinum and gold surfaces (0.11 and 0.56, respectively).

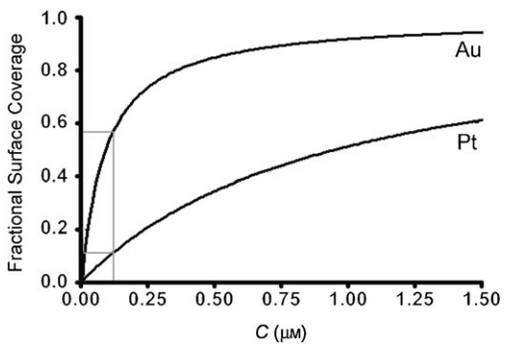

Figure 3. The steady-state fractional surface coverage $\theta(\infty)$ of gold and platinum surfaces as a function of 3R-GBP1 concentration (C). The gray line corresponds to the 0.12-μM (0.5 μg mL^{-1}) 3R-GBP1 concentration.

2.2. Cross-Specificity of a Gold-Binding Peptide: Gold versus Platinum Substrates

Knowledge of the adsorption-kinetics parameters of an inorganic-binding peptide on a given material, other than on the material for which the peptide was selected, is significant in applications that require comparative peptide stability. These applications may include cases of the peptide as a linker and erector in assembly or as a growth modifier in biofabrication. In the previous section, we established the parameters of the kinetics as well as the binding stability of a gold-binding peptide on platinum, a noble metal comparatively similar to the originally selected material, gold. There are also other potential utilizations of these biomimetic molecules that may require selective adsorption of inorganic-binding peptides on various inorganic entities; examples include in the development of molecularly functionalized surfaces (e.g., cell immobilization or cell sorting), in the development of biocompatible surfaces,[14–16] and in applications of directed immobilization or assembly of nanoparticles or nanowires on various inorganic substrates or pads.[27–28]

Here we demonstrate the specific immobilization of gold-binding peptides on gold compared to two different platforms. A comparison was made with both SiO_2 (25 nm, grown via dry oxidation on a silicon wafer) and another metal, platinum, in a selective environment. In the first case, we prepared gold micropatterns in the form of 5-μm-wide lines on the SiO_2-coated wafer, creating alternate Au/SiO_2 strips as shown in the optical microscope image in Figure 4a. To demonstrate the directed assembly of a gold-binding peptide on Au strips as compared to the bare SiO_2 substrate regions, we used SAQDs (red-light emitting) that are preferentially immobilized on GBP1. To accomplish this, we biotinylated GBP1 (bio-GBP1) and incubated the Au-strip-patterned substrate with the functionalized peptide (0.5 μg mL^{-1}) for two hours. It was expected that because of the strong and specific biotin–streptavidin conjugation, the QDs would be immobilized on the GBP1 and thereby delin-

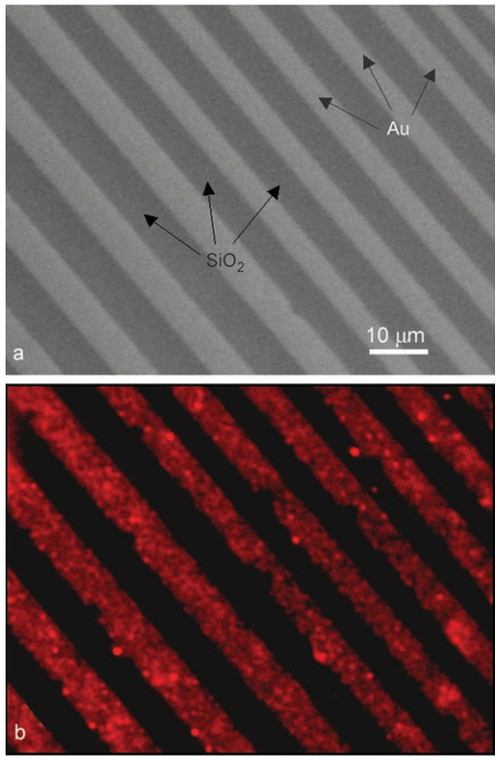

Figure 4. a) Optical microscopy image of gold strips micropatterned on a SiO_2 substrate. b) Fluorescence microscopy image of the assembled streptavidin-coated quantum dots on self-immobilized bio-GBP1 on the gold strips only.

eate the gold regions. Figure 4b is an image taken with a fluorescence microscope using an appropriate filter to record the red-light emission; this reveals the Au strips where the bio-GBP1 was originally assembled; no color reversal was observed in the SiO_2 regions. Figure 5c–e schematically demonstrates the procedure.

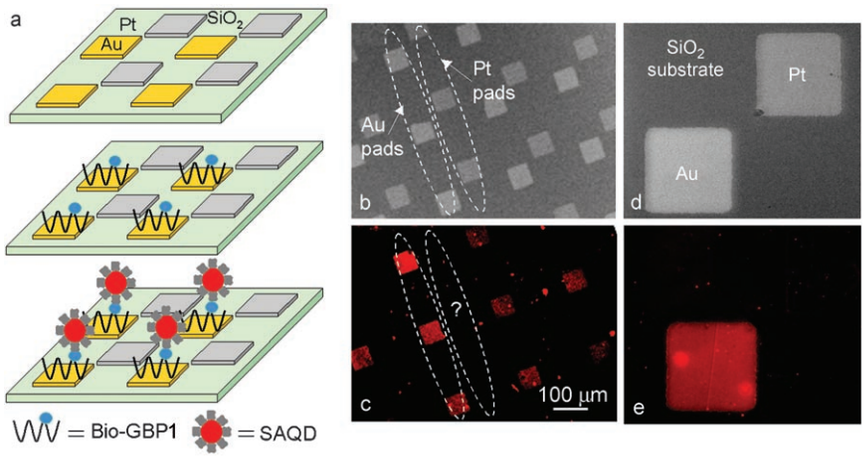

Figure 5. a) Schematic illustration of the directed self-assembly of SAQDs on bio-GBP1 only on the gold regions of a silicon dioxide substrate containing both gold and platinum pads. The micrographs in (b) and (d) are optical microscopy images of the microfabricated template for the self-assembly experiments, showing the adjacent gold and platinum pads before peptide immobilization. The fluorescent images in (c) and (e) (low and high magnification, respectively) reveal SAQD immobilization on the self-assembled bio-GBP1, verifying the selective binding of the polypeptide to the gold regions only.

The above results show that a peptide originally genetically selected and engineered to bind to gold does indeed bind preferentially to gold regions even in the presence of another biological linker (i.e., biotin) and on the micropatterned surface of an oxidized silicon wafer; this demonstrates the cross-specificity of a metal-binding peptide between a metal and an oxide. A more dramatic demonstration of the selectivity of metal-binding peptides is to show its preference for one of two metals when both are micropatterned on the same SiO_2-covered wafer. Figure 5 shows the schematic process of pattern preparation on a silicon oxide surface covered with alternating gold and platinum squares with 100-μm long edges. To prepare the patterned template (Figure 5a) the silicon surface was thermally oxidized to form a thin silicon dioxide film (25 nm) onto which first gold and then platinum was sputter-deposited by means of photoresist patterning and lift-off to create the alternating metal squares (see Experimental Section). The microfabricated template is shown in Figure 5b and c; the brighter squares are the patterned gold and platinum regions on the oxide substrate. To demonstrate the directed assembly of a gold-binding peptide on Au squares compared to the Pt regions, we used SAQDs that were preferentially immobilized on the GBP1, therefore delineating the gold regions. To accomplish this, we biotinylated GBP1 and incubated the functionalized peptide ($0.5\ \mu g\,mL^{-1}$) for two hours with the substrate containing both metal patterns. At this point, it was not clear whether the bio-GBP1 was immobilized on both metal regions or just on the gold-patterned areas. After appropriate washing to remove any excess or nonspecific binding of the peptide on the metal regions, SAQDs were added to the solution containing the microtemplated bio-GBP1 immobilized substrate. As shown in the fluorescence microscopy images in Figure 5d and e, only one set of the patterned squares appears red, demonstrating that the regions of one metal (confirmed to be gold by energy dispersive X-ray microanalysis; data not shown) immobilize the quantum dots. The immobilization of the quantum dots on the patterned gold regions was, therefore, accomplished through the streptavidin (on QDs) to biotin (on GBP1) link. Here, the peptides specifically recognize the gold surface and are self-organized; they then direct the immobilization of nanoscale entities (10-nm QDs) onto predefined locations. In summary, this two-stage protocol demonstrates two significant issues in nanobiotechnology. Firstly, that a combinatorially selected and genetically engineered inorganic-binding peptide preferentially assembles on its original, selective material even in the presence of another, similar material. Secondly, inorganic-binding peptides can be used as highly functional molecular erectors to direct the immobilization of nanoscale objects (e.g., QDs)

NANO MICRO small

preferentially over one patterned region of a material (Au) compared to another (Pt), both on the same substrate (SiO_2).

At this point, the mechanism by which a peptide binds selectively to a metal surface rather than an oxide surface, and, more significantly, how a peptide can choose between two very similar noble metals (Au and Pt), is not well understood. A recent NMR study indicates that GBP1 has an open cyclic molecular structure with its three repeat units each consisting of 14 amino acid domains.[29] Although the exact mechanism of inorganic recognition by peptides is of considerable interest[12–14] and the subject of future studies, for now it is sufficient to argue that the polar moieties on the GBP1 as well as the physical conformation of the polypeptide may be responsible for the specific adsorption onto gold rather than either silica or platinum.[30] This is unlike the thiol-based molecular binding systems where S forms strong bonds with the metal substrate (e.g., Au, Ag, Pt, or Pd) leading to the self-assembly of these noble metals.[31–32]

3. Conclusions

Engineered polypeptides have already been recognized as having material-specific binding properties;[6–9,33] our result is the first quantitative demonstration that a genetically engineered peptide has metal-specific binding and recognition properties. This result is significant in its sophistication in bridging the biological and inorganic domains in terms of distinguishing not only between two materials but also between two very similar noble metals (Au and Pt). The metal specificity of a peptide could be utilized in guiding the self-assembly of structures applicable in many areas of nano- and microtechnology. In particular, the result of directed immobilization of quantum dots on a desired metal (Au) as opposed to another (Pt), both being micropatterned on a silicon wafer, would provide a new complexity in developing platforms that are required in utilizing multiprobe and target interactions using Si-based biosensors.

Both noble metals, gold and platinum, have traditional as well as recently developed technological uses including electronics, sensors, catalysis, and in medicine.[14,34,35] Both metals are chemically stable and resistive to oxidation but have significantly different mechanical properties and biocompatibilities; gold is heavily used as a biocompatible material as, for example, coatings on therapeutic devices such as stents, while platinum, in addition to being an excellent catalyst, is used in cancer therapy due to its controlled toxicity.[14,36] Both metals also constitute the major elements used in nanotechnological systems, in particular in the development of concepts and applications involving conductors, size- and scale-related electronic and photonic properties, and as substrates for developing self-assembled molecular systems. The strong binding and stability seen here demonstrate that a gold-binding peptide could be used as a binding agent, molecular linker, or a substrate bound specifically to gold under aqueous and biocompatible conditions. In particular, the concentration-tunable specificity between gold and platinum would allow use in, for example, controlled drug delivery and release. Finally, the quantitative peptide affinity to a metal and its specificity against other metals of practical interest are significant for use of these engineered biomolecular systems in creating biologically viable and technologically accessible genetically functionalized surfaces and linkers in a wide variety of nanobiotechnological applications.[14–16,36,37] New alternatives are now offered in a field that has so far been dominated by self-assembled monolayers, particularly by thiol- or silane-based linkages.[31,32,38]

4. Experimental Section

Gold-binding protein: The high-purity (95%) synthesized form of the 3-repeat of GBP1 (originally designed in our laboratory) was purchased from United Biochemical Research Inc. (Seattle, WA). The concentrations of the GBP1 solutions, ranging from 0.5 to 6 $\mu g\,mL^{-1}$, were prepared in a 10 mM phosphate buffer (3:1 K_2HPO_4: KH_2PO_4) containing 100 mM of KCl. Binding experiments under neutral conditions were carried out with a 10 mM phosphate carbonate (PC) buffer (pH 7.2) containing 100 mM of KCl. Nanopure Milli-Q water was used in preparing all the solutions unless stated otherwise.

Binding experiments: AT-cut (zero frequency dependence on temperature) QCM electrodes with a fundamental resonant frequency of 10 MHz were obtained from International Crystal Manufacturing Co. (Oklahoma City, OK). The crystals were coated on both sides with approximately 100 Å of Cr and 1000 Å of metal (gold or platinum). The crystal surfaces were optically polished. The diameter of the crystals and electrodes were 8.8 and 5.0 mm, respectively. The electronic oscillator circuit was a typical Colpits oscillator, which had a buffer amplifier. A 12-V DC current was applied to the oscillator circuit to drive the crystal and the frequency was measured with a Hewlett–Packard frequency counter (model number 53131 A 225 Hz Universal Counter, Agilent Technologies, USA).

In real-time adsorption measurements, a sufficient amount of GBP1 buffer solution was introduced into the cell until a stable baseline was obtained and the GBP1 solution was subsequently added. The frequency change of the crystal in the pure buffer solution was recorded for 30–60 min. Following a stable baseline, the required amount of GBP1 solution was added into the cell to obtain the desired concentration, and the frequency change was recorded continuously during the adsorption process. For the adsorption onto the gold surface, four different concentrations, varying from 1.0 to 4 $\mu g\,mL^{-1}$, were studied, whereas GBP1 binding onto the platinum surface was studied at five concentrations ranging from 1.0 to 6 $\mu g\,mL^{-1}$.

Self-assembly on microfabricated patterns: To prepare the patterned template, the silicon wafer surface was thermally oxidized to form a thin silicon dioxide film (25 nm, grown with dry oxidation). This oxide surface was then patterned using photolithography; deposition via sputtering of TiW (10 nm) and then Au (25 nm) was followed by lift-off of the photoresist to form the gold pattern (Figure 4 a). The process of photolithography, evaporation, and lift-off was repeated to form a pattern of platinum

squares (25-nm Pt film over a 10-nm Ti adhesion layer) adjacent to those made of gold on the silicon dioxide surface.

Biotinylated 3R-GBP1 was used to demonstrate the guided self-assembly of quantum dots. To immobilize the bio-GBP1, the substrate was incubated in a 0.5 $\mu g\,mL^{-1}$ buffered solution of bio-GPB1 for two hours. The buffer solution contained 10 mM potassium phosphate and 0.1 M potassium chloride (pH 7.2). This step allowed for the preferential self-assembly and binding of bio-GBP1 onto the Au pattern on the substrate. SAQDs were used for the directed-assembly experiments. These were CdSe/ZnS nanoshells, size-controlled to be red in color and chemically functionalized to be conjugated with SA (QD605, Quantum Dot Corporation). The substrate was incubated for 45 min with the quantum dots in the buffered bio-GPB1 solution with a concentration of 1:10 v/v. The quantum dots were then selectively self-assembled to bio-GBP1 on Au via the strong biotin-streptavidin link; they could then be imaged with a fluorescence microscope using Qdot605 with a 20-nm emission filter (Chroma Technology Corp., Rockingham, USA); see Figure 4).

Acknowledgements

This research was funded by the US Army Research Office through a DURINT (Defense University Research Initiative on Nanotechnology) Program, NSF through the Genetically Engineered Materials Science and Engineering Center (GEMSEC), and the NIH through the Center of Excellence in Genome Science (Microscale Life Science Center), all at the University of Washington.

[1] *Biomimetic Materials Chemistry* (Ed.: S. Mann), VCH, New York, **1996**.
[2] *Hierarchically Structured Materials* (Eds.: I. A. Aksay, E. Baer, D. Tirrell, M. Sarikaya) Vol. 254, Materials Research Society, Pittsburgh, **1994**.
[3] M. Sarikaya, *Proc. Natl. Acad. Sci. USA* **1999**, *96*, 14183–14185.
[4] C. Sanchez, H. Arribart, M. M. G. Guille, *Nat. Mater.* **2005**, *4*, 277–288.
[5] S. Zhang, *Nat. Biotechnol.* **2003**, *21*, 1171–1173.
[6] M. Sarikaya, C. Tamerler, A. Y. Jen, K. Schulten, F. Baneyx, *Nat. Mater.* **2003**, *2*, 577–585.
[7] S. R. Whaley, D. S. English, E. L. Hu, P. F. Barbara, A. M. Belcher, *Nature* **2000**, *405*, 665–668.
[8] R. R. Naik, S. J. Stringer, G. Agarwal, *Nat. Mater.* **2002**, *1*, 169–172.
[9] C. K. Thai, H. X. Dai, M. S. R. Sastry, M. Sarikaya, D. T. Schwartz, F. Baneyx, *Biotechnol. Bioeng.* **2004**, *87*, 129–137.
[10] K. I. Sano, H. Sasaki, K. Shiba, *Langmuir* **2005**, *21*, 3090–3095.
[11] S. Brown, M. Sarikaya, E. Johnson, *J. Mol. Biol.* **2000**, *299*, 725–735.
[12] J. J. Gray, *Curr. Opin. Sruct. Biol.* **2004**, *14*, 110–115.
[13] K. Nakanishi, T. Sakiyama, K. Imamura, *J. Biosci. Bioeng.* **2001**, *91*, 233–244.
[14] *Biomaterials Science: An Introduction to Materials in Medicine* (Eds.: B. Ratner, F. Schoen, A. Hoffman, J. Lemons), Academic, San Diego, **1996**.
[15] G. MacBeath, S. L. Schreiber, *Science* **2000**, *289*, 1760–1763.
[16] U. Reineke, R. Volkmar-Engert, J. Sneider-Mergener, *Curr. Opin. Biotechnol.* **2001**, *12*, 59–64.
[17] D. H Min, M. Mrksich, *Curr. Opin. Chem. Biol.* **2004**, *8*, 554–558.
[18] B. S. Murray, C. Deshaires, *J. Colloid Interface Sci.* **2000**, *227*, 32–41.
[19] J. Rickert, A. Brecht, W. Göpel, *Biosens. Bioelectron.* **1997**, *12*, 567–575.
[20] F. Höök, M. Rodahl, P. Brzezinski, B. Kasemo, *Langmuir* **1998**, *14*, 729–734.
[21] L. E. Bailey, D. Kambhampati, K. K. Kanazawa, W. Knoll, C. Frank, *Langmuir* **2002**, *18*, 479–489.
[22] G. Sauerbrey, *Z. Phys.* **1959**, *155*, 206–222.
[23] H. M. Schessler, D. S. Karpovich, G. J. Blanchard, *J. Am. Chem. Soc.* **1996**, *118*, 9645–9651.
[24] P. Ihalainen, J. Peltonen, *Sens. Actuators B* **2004**, *102*, 207–218.
[25] K. A. Marx, *Biomacromolecules* **2003**, *4*, 1099–1120.
[26] D. S. Karpovich, G. J. Blanchard, *Langmuir* **1994**, *10*, 3315–3322.
[27] S. R. Nicewarner-Peña, R. G. Freeman, B. D. Reiss, L. He, D. J. Peña, I. D. Walton, R. Cromer, C. D. Keating, M. J. Natan, *Science* **2001**, *294*, 137–141.
[28] W. F. Paxton, K. C. Kistler, C. C. Olmeda, A. Sen, S. K. St. Angelo, Y. Cao, T. E. Mallouk, P. Lammert, V. H. Crespi, *J. Am. Chem. Soc.* **2004**, *126*, 13424–13431.
[29] R. Braun, M. Sarikaya, K. S. Schulten, *J. Biomater. Sci. Polym. Ed.* **2002**, *13*, 747–757.
[30] E. E. Oren, C. Tamerler, M. Sarikaya, *Nano Lett.* **2005**, *5*, 415–419.
[31] G. M. Whitesides, J. P. Mathias, C. T. Seto, *Science* **1991**, *254*, 1312–1319.
[32] F. Schreiber, *Prog. Surf. Sci.* **2000**, *65*, 151–257.
[33] K. Goede, P. Busch, M. Grundmann, *Nano Lett.* **2004**, *4*, 2115–2120.
[34] T. W. Ellis, *Gold Bull.* **2004**, *37*, 66–71.
[35] A. P. Murphy, *J. Met.* **2001**, *53*, 11–13.
[36] S. E. Sakiyama-Elbert, J. A. Hubbell, *Ann. Rev. Mater. Res.* **2001**, *31*,183–201.
[37] T. Velten, H. H. Ruff, D. Barrow, N. Aspragathos, P. Lazarou, E. Jung, C. K. Malek, M. Richter, J. Kruckow, *IEEE Trans. Adv. Packag,* **2005**, *28*, 533–546.
[38] B. H. Lee, T. Nagamune, *Biotechnol. Bioprocess Eng.* **2004**, *9*, 69–75.

Received: February 8, 2006
Published online on September 8, 2006

